

A Kinetic Study on the Autocatalytic Cure Reaction of a Cyanate Ester Resin

Ching-Chung Chen, Trong-Ming Don, Tai-Hung Lin, Liao-Ping Cheng

Department of Chemical and Materials Engineering, Tamkang University, Tamsui, Taipei County, 25147, Taiwan

Received 30 September 2003; accepted 22 January 2004

ABSTRACT: The cure of a novolac-type cyanate ester monomer, which reacts to form a polycyanurate network, was investigated by using differential scanning calorimeter. The conversions and the rates of cure were determined from the exothermic curves at several isothermal temperatures (513–553 K). The experimental data, showing an autocatalytic behavior, conforms to the kinetic model proposed by Kamal, which includes two reaction orders, m and n , and two rate constants, k_1 and k_2 . These kinetic parameters for each curing temperature were obtained by using Kenny's graphic-analytical technique. The overall reaction order was about 1.99 ($m = 0.99$, $n = 1.0$) and the activation energies for the rate constants, k_1 and k_2 , were 80.9 and 82.3 kJ/mol, respectively. The results show that the autocatalytic model

predicted the curing kinetics very well at high curing temperatures. However, at low curing temperatures, deviation from experimental data was observed after gelation occurred. The kinetic model was, therefore, modified to predict the cure kinetics over the whole range of conversion. After modification, the overall reaction order slightly decreased to be 1.94 ($m = 0.95$, $n = 0.99$), and the activation energies for the rate constants, k_1 and k_2 , were found to be 86.4 and 80.2 kJ/mol. © 2004 Wiley Periodicals, Inc. *J Appl Polym Sci* 92: 3067–3079, 2004

Key words: differential scanning calorimetry (DSC); activation energy; curing of polymers

INTRODUCTION

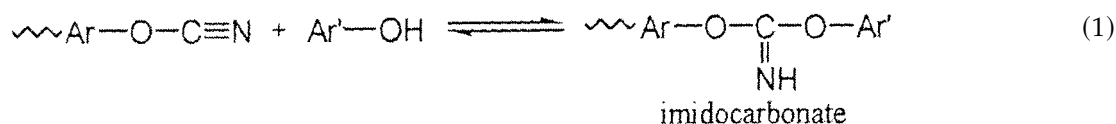
Cyanate ester resin has drawn a great deal of attention as one of the high-performance thermosets, comparable to epoxies and polyimides. After heating, the cyanate ester monomer undergoes self-cyclotrimerization to form a three-dimensional network structure of polycyanurate.¹ Polycyanurate possesses several superior properties including high glass-transition temperature, low moisture absorption, low dielectric constant, good thermal stability, low shrinkage, and strong adhesion to metal. It is widely used in the fields of electrical and aero industries: for example, as a major component in the printed circuit board, encapsulates fibers, coatings, and adhesives.¹ In addition, polycyanurate can be processed with the addition of other thermoplastics or even thermosets, such as epoxies,^{2–4} bismaleimide,⁵ phenol-formaldehyde,⁶ polysulfone,⁷ and poly(propylene oxide)⁸ to yield blends with unique properties. After curing in the presence of a second polymer, a well-compatible blend or an in-

terpenetrating network structure can be formed, which often demonstrates improved toughness compared with pure polycyanurate. Polycyanurate becomes brittle at very high conversions.⁹

Bauer et al.¹⁰ found that pure cyanate ester monomer did not undergo polymerization even at high temperatures. This reaction must be catalyzed by water or phenol compounds. Generally, in the commercial production of cyanate ester monomer, about 0.5–1.5 mol % of phenol impurity is found to be present in the resin and hardly can be removed by ordinary separation methods. This phenol impurity acts as a catalyst for subsequent cyclotrimerization reactions. A lot of effort thus goes into purifying the cyanate ester resins so that they have adequate shelf life and can be cured under controlled and reproducible conditions. During curing at elevated temperatures, three monomer molecules may undergo cyclotrimerization to form cyanurate (or triazine ring). If a multifunctional cyanate ester resin is initially used, the triazine ring can continue to react with other monomers and eventually a three-dimensional network structure of polycyanurate is produced.¹ A three-step mechanism was proposed for the formation of cyanurate from cyanate ester monomer being catalyzed by phenol.^{10–12} First, the $—O—C≡N$ group reacts with phenol to form imidocarbonate:

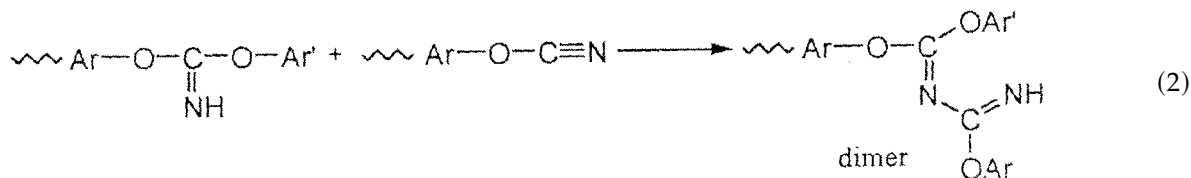
Correspondence to: T.-M. Don (tmdon@mail.tku.edu.tw).

Contract grant sponsor: National Science Council, Taiwan, Republic of China; contract grant number: NSC 91-2622-E-032-001-CC3.



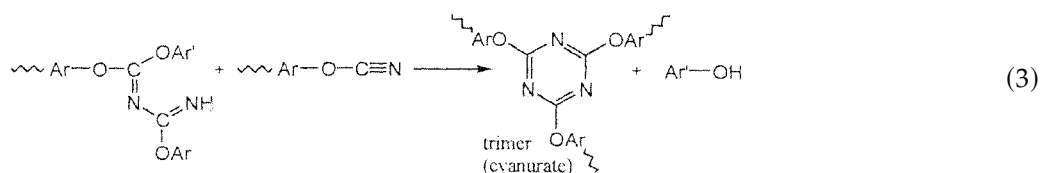
where Ar is a phenyl group and Ar'—OH is phenol. In the second step, imidocarbonate continues to react

with the —O—C≡N functional group to form a dimer,



Finally, the dimer reacts with another —O—C≡N group to produce a trimer (i.e., cyanurate), together

with the release of a phenol,



According to the previous reaction scheme, the cure of cyanate ester resin can be considered as the formation of a triazine from three —O—C≡N functional groups,



where C is cyanate ester monomer; T is triazine; and P is phenol.

It has been proved¹⁰⁻¹² that the produced triazine can catalyze the reaction itself (i.e., an autocatalytic reaction). Therefore, the rate equation can be described in the form

$$-\frac{d[\text{C}]}{dt} = k''[\text{C}]^n[\text{T}]^m[\text{P}]^l \quad (5)$$

where [C] is concentration of cyanate ester monomer; [T] is concentration of triazine; [P] is concentration of phenol; k'' is the rate constant; and m , n , and l are the reaction orders.

The rate equation can also be expressed in terms of the monomer conversion, α ,

$$[\text{C}] = [\text{C}]_0(1 - \alpha) \quad (6)$$

$$[\text{T}] = 1/3[\text{C}]_0\alpha \quad (7)$$

where $[\text{C}]_0$ is the initial concentration of cyanate ester monomer.

Substitution of eqs. (6) and (7) into eq. (5) gives

$$\frac{d\alpha}{dt} = k''[\text{P}]^l(1/3)^m[\text{C}]_0^{m+n-1}\alpha^m(1 - \alpha)^n \quad (8)$$

Because phenol acted as a catalyst and the concentrations of the intermediates were assumed to be very small, a steady-state approximation was thus assumed (i.e., both $[\text{C}]_0$ and $[\text{P}]$ were taken to be constants). This is a very reasonable assumption that will simplify the kinetic equations derived from the complex reaction mechanism. As a result, eq. (8) can be further reduced to a simpler form,

$$\frac{d\alpha}{dt} = k_2\alpha^m(1 - \alpha)^n \quad (9)$$

where k_2 is a constant equal to $k''[\text{P}]^l(1/3)^m[\text{C}]_0^{m+n-1}$. Equation (9) is thus used to describe autocatalytic reactions, which can reach their maximum reaction rate at 30 to 40% of conversion. In the literature,¹³⁻¹⁷

this equation was widely used in the cure kinetics of epoxy resins. To decrease the cure temperature of cyanate ester resin for the purpose of cost reduction, metal ions are generally employed to catalyze the reaction, such as magnesium, zinc, copper, cobalt, chromium, manganese, iron, aluminum, and titanium.^{18–25} Simon and Gillham¹² and other researchers²² pointed out that the metal ion could form ionic complex with the imidocarbonate, which in turn accelerated the reaction. If an appreciable amount of external catalyst was added into the system, the autocatalytic reaction would be suppressed and the overall reaction becomes



where M is the ion-complexed imidocarbonate.

The rate equation corresponding to eq. (10) is given by

$$-\frac{d[C]}{dt} = k'[C]^n[M]^o[P]^l \quad (11)$$

where k' is the rate constant and o is the reaction order.

In a way similar to obtaining eq. (8), eq. (11) is converted to a form in terms of the conversion

$$\frac{d\alpha}{dt} = k'[M]^o[P]^l[C]_0^{n-1}(1-\alpha)^n \quad (12)$$

Because $[M]$, $[P]$, and $[C]_0$ are all constants, eq. (12) can be expressed in a succinct form

$$\frac{d\alpha}{dt} = k_1(1-\alpha)^n \quad (13)$$

where constant k_1 is equal to $k'[M]^o[P]^l[C]_0^{n-1}$. Equation (13) is generally ascribed to an n th-order reaction in thermoset cure kinetics, and the reaction exhibits its maximum reaction rate at the beginning of cure. If both the external catalytic and the autocatalytic reactions were considered, eqs. (9) and (13) can be combined to yield

$$\frac{d\alpha}{dt} = (k_1 + k_2\alpha^m)(1-\alpha)^n \quad (14)$$

Equation (14) was originally proposed by Kamal²⁶ as a semiempirical equation to describe the cure kinetics of epoxies. Since then, this equation was widely used in the cure kinetics of epoxy resins and unsaturated polyester.^{26–35} After knowing the values of k_1 , k_2 , m , and n , the relationship between the cure time and conversion can be obtained by the integration of eq. (14)

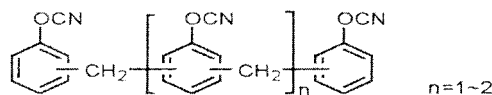
$$t = \int_0^\alpha \frac{d\alpha}{(k_1 + k_2\alpha^m)(1-\alpha)^n} \quad (15)$$

A differential scanning calorimeter (DSC) has frequently been used in studying the cure kinetics of thermosets, because it is very sensitive and reliable, and only small amounts of material are required. Therefore, it is the purpose of this article to use DSC to study the cure kinetics of a multifunctional cyanate ester monomer, PT30. In addition, Kenny's graphic-analytical technique^{27,28} was used to obtain the kinetic parameters of the rate equation. These kinetic parameters were then compared with the values reported in the literature.

EXPERIMENTAL

Materials

The cyanate ester resin, PT30, supplied by Lonza Co., is a novolac-type resin. The molecular weight is over the range of 320 to 420 g/mol and the specific gravity is 1.25. The structure is illustrated below.



The curing reaction was studied by using a DSC 7 from Perkin-Elmer. The instrument was first calibrated with pure indium in terms of the temperature and enthalpy. About 5 mg of the PT30 monomer was put into an aluminum pan and heated to a predetermined temperature at a heating rate of 100 K/min. The temperature was held constant throughout the isothermal cure reaction and the heat of reaction was recorded with time. The isothermal cure reaction was studied at 513, 523, 533, 543 and 553 K. After no more heat of reaction was released at this constant temperature, the sample was cooled down to 303 K and reheated to 623 K at a rate of 10 K/min. An additional exothermic peak might be observed at high temperature region, and the residual heat of reaction was thus calculated from the area under the peak.

Fourier transform infrared spectrophotometer, Magna-IR 550 (Nicolet) was used to characterize the chemical structure of cyanate ester resin PT30 (supplied by Lonza Co., Basel, Switzerland; novolac-type resin) before and after cure. The cyanate ester resin was dissolved in acetone first and then cast onto KBr disc. The disc was put into a desiccator followed by vacuum drying to remove the acetone. For the sample after cure, cyanate ester resin being converted into polycyanurate, it was ground into powder first and then homogeneously mixed with a 50-fold quantity of KBr powder. The mixture was subsequently pressed

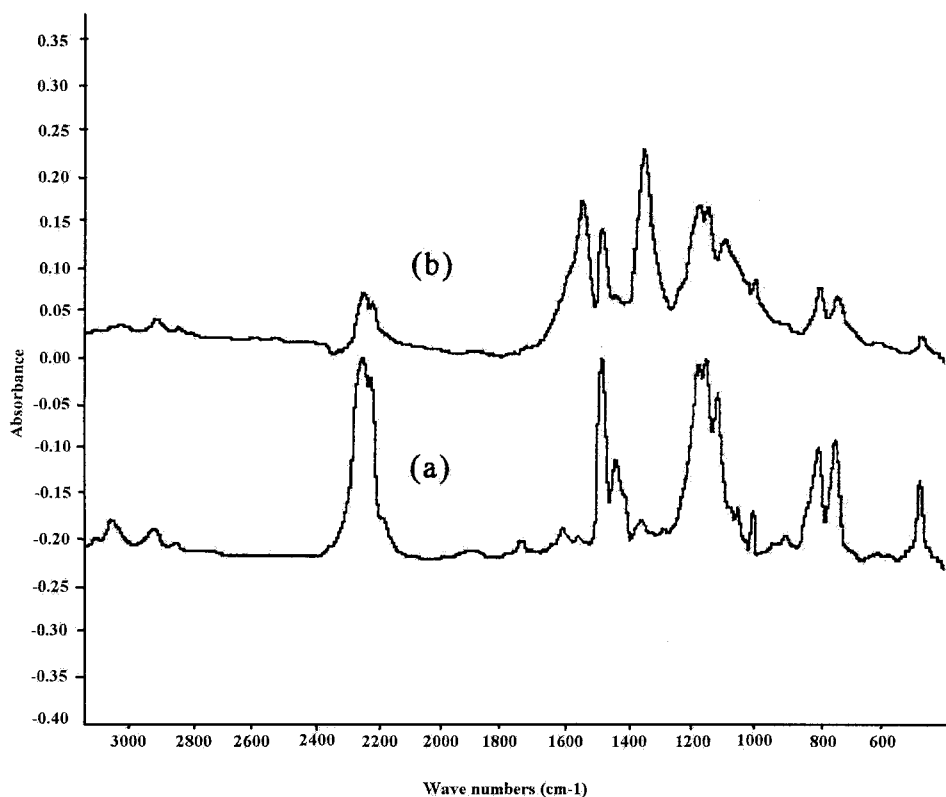


Figure 1 FTIR spectra of PT30 cyanate ester resin before (a) and after (b) cure at 523 K for 5 min.

into a disc for FTIR measurement from 4000 to 400 cm^{-1} . The resolution was set at 4 cm^{-1} and 32 scans were taken to average the signal. Thermal stability of the cured polycyanurate was investigated by using a thermal gravimetric analyzer, TGA 2950 (TA Co.). About 5 mg of the polycyanurate sample, which had been cured at 523 K for 10 min, was heated from 303 to 1000 K at a heating rate of 10 K/min, and the mass of the sample was recorded continuously.

RESULTS AND DISCUSSION

Structure characterization

Figure 1 shows the FTIR spectra of a cyanate ester resin PT30 before and after cure at 523 K for 5 min. A very small peak at 1750 cm^{-1} was observed, which was caused by the absorption of the intermediate, imidocarbonate, from the catalytic reaction of $\text{—O—C}\equiv\text{N}$ group with the phenol impurity accompanying the cyanate ester monomer. After cure, the absorption peak at 2266 cm^{-1} corresponding to the cyanate ester monomer $\text{—O—C}\equiv\text{N}$ decreased greatly. In contrast, the characteristic peaks of the produced polycyanurate from triazine ring at 1563 and 1366 cm^{-1} were clearly observed. The absorption peaks at 2930 and 1500 cm^{-1} being assigned to the stretching vibration of CH_2 group bridging the phenyl rings and the phenyl

ring itself, respectively, were used as the internal reference, as they were not involved in the cure reaction.

Cure kinetics studied by DSC

The cure reaction of the cyanate ester resin is exothermic and can be conveniently monitored by DSC. The isothermal cure reaction was investigated at several temperatures from 513 to 553 K with a 10 K interval. Figure 2 shows the evolved exothermic curves at these temperatures. The heat of reaction $Q_T(t)$ after a certain time is $Q_T(t) = \int_0^t (dQ/dt)dt$, where dQ/dt is the exothermic heat per unit time per unit mass of resin (W/g). Consequently, the final heat of reaction, $Q_T(t_f)$, at each temperature, was calculated from the integrated area under the curve from the beginning to the end of the reaction (t_f) (i.e., $Q_T(t_f) = \int_0^{t_f} (dQ/dt)dt$). The results are listed in Table I. It appears that the higher the cure temperature, the larger the final heat of reaction.

During the cure, the resin viscosity increased with time due to the increase of its molecular weight. At a certain conversion, the system started to gel, where the reaction rate was controlled by diffusion because of the very high viscosity in the matrix. For the cyanate ester resin, the gel point was estimated at the conversion between 0.5 and 0.63.^{36,37} Finally, a vitrifi-

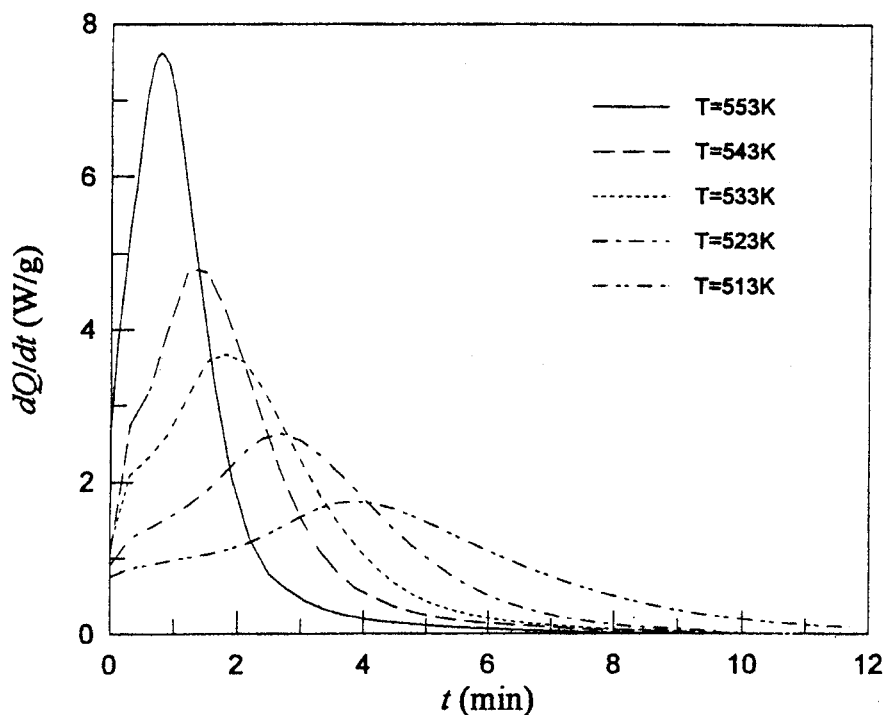


Figure 2 Isothermal exothermic curves of PT30 cyanate ester resin cured at different temperatures in DSC experiments.

cation state was reached, where the glass transition temperature (T_g) of the cured resin exceeded the cure temperature. At this point, no further reaction was observed, unless the cure temperature was raised higher than the T_g of the cured resin. Therefore, the polycyanurate resin after isothermal cure was cooled down to 303 K and reheated to 623 K at 10 K/min for the determination of the residual heat of reaction, $Q_{T,R}$. The dynamic thermal scan in DSC to 623 K did not cause any thermal decomposition of the cured polycyanurate, as confirmed by the TGA experiment.

TABLE I
The Curing Reaction Data of a Cyanate Ester Resin,
PT30, Calculated from Exothermic Curves in DSC
(Samples Were Isothermally Cured at
Different Temperatures)

	Temperature (K)				
	513	523	533	543	553
$Q_T(t_f)$ (J/g)	581.01	600.46	622.48	642.65	655.77
$Q_{T,R}$ (J/g)	84.12	67.67	50.56	33.14	13.84
$Q_T(t_f) + Q_{T,R}$ (J/g)	665.13	668.13	673.04	675.79	669.61
t_f (min)	12.85	9.64	7.34	6.31	4.48
α_{\max}	0.87	0.90	0.92	0.95	0.98
t_{Peak} (min)	4.14	2.86	1.89	1.34	0.88
α_{Peak}	0.41	0.40	0.39	0.40	0.39

$Q_T(t_f)$: isothermal heat of reaction; $Q_{T,R}$: residual heat of reaction; $Q_T(t_f) + Q_{T,R}$: total heat of reaction; t_f : the reaction time at the end of cure; α_{\max} : maximum conversion; t_{Peak} : the reaction time at the exothermic peak; α_{Peak} : the conversion at the exothermic peak.

The on-set decomposition temperature was 670 K. The calculated $Q_{T,R}$ values are also listed in Table I. The residual heat of reaction was found to decrease with the cure temperature. The total heat of reaction was by definition equal to $Q_T(t_f) + Q_{T,R}$. As shown in Table I, it almost did not change with the cure temperature from 513 to 553 K. The average value of total heat of reaction at these temperatures was 670 J/g, corresponding to -88 kJ per equivalent cyanate group, if a cyanate functional group equivalent weight is assumed to be equal to that of the resin repeat unit (131 g/equiv). If the conversion of reaction (α) was assumed to be proportional to the heat of reaction, then the conversion at a specific time can be determined from the equation:

$$\alpha = \frac{Q_T(t)}{Q_T(t_f) + Q_{T,R}} \quad (16)$$

The maximum conversion α_{\max} at a certain cure temperature was the conversion when there was no further heat released and therefore was defined as

$$\alpha_{\max} = \frac{Q_T(t_f)}{Q_T(t_f) + Q_{T,R}} \quad (17)$$

The time at the end of reaction (t_f), the maximum conversion (α_{\max}), the time at the exothermic peak (t_{Peak}), and the corresponding conversion (α_{Peak}) for curing at different temperatures are all listed in Table

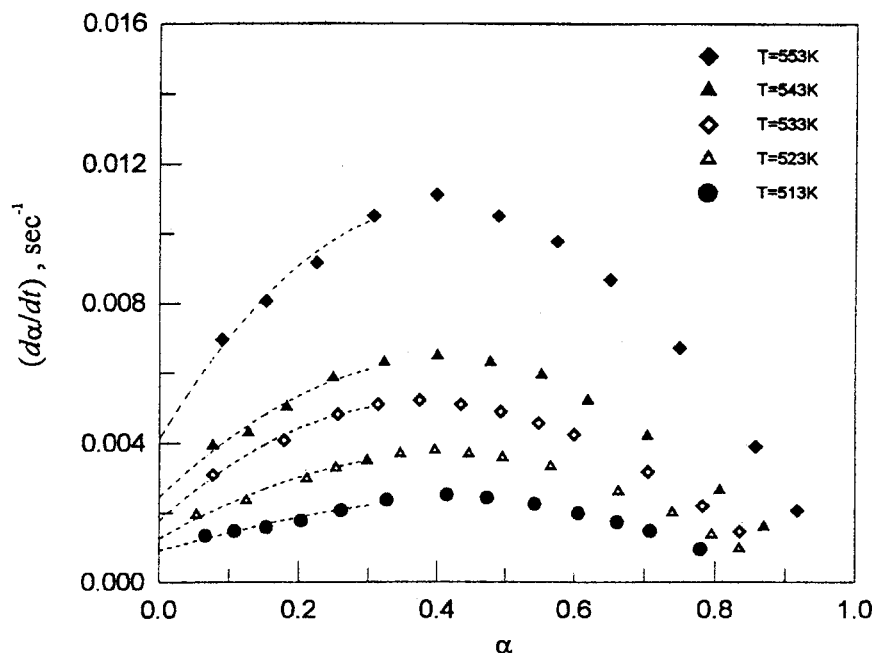


Figure 3 The reaction rate as a function of conversion of PT30 cyanate ester resin at several curing temperatures.

I. The maximum conversion increased with cure temperature, which is in accordance with the final heat of reaction. The calculated maximum conversion at 513 K was 0.87 and it increased to 0.98 at 553 K, a state of almost complete reaction. When eqs. (16) and (17) were combined, a relationship between α and α_{\max} can be obtained

$$\alpha = \frac{Q_T(t)}{Q_T(t_f)} \alpha_{\max} = \frac{\int_0^t \left(\frac{dQ}{dt}\right) dt}{Q_T(t_f)} \alpha_{\max} \quad (18)$$

Both $Q_T(t_f)$ and α_{\max} were only dependent on cure temperature. Therefore, when the above equation was differentiated with respect to time, the rate of change of conversion (i.e., the reaction rate) can be expressed as:

$$\frac{d\alpha}{dt} = \frac{d \int_0^t \left(\frac{dQ}{dt}\right) dt}{dt} \frac{\alpha_{\max}}{Q_T(t_f)} = \frac{dQ}{dt} \frac{\alpha_{\max}}{Q_T(t_f)} \quad (19)$$

The conversion (α) and the corresponding reaction rate ($d\alpha/dt$) were thus calculated from the above equations. Figure 3 shows the reaction rate as a function of conversion at different cure temperatures. For all cases, the reaction rate increased with conversion until it reached a maximum. At this point, the conversion was ~ 0.40 . This is in accordance with the characteristic of an autocatalytic reaction, where the maximum rate occurs at a conversion between 0.3 and 0.4.

Kenny's graphical analysis^{27,28}

It is difficult to obtain the reaction parameters, k_1 , k_2 , m , and n , in the rate equation given by eq. (14). Kenny et al.^{27,28} proposed a graphic-analytical technique to solve this equation, which has been demonstrated to be very convenient yet with sufficient accuracy.^{16,35}

Determination of rate constant k_1

In eq. (14), when the conversion α approaches zero, the rate constant k_1 can be obtained

$$\lim_{\alpha \rightarrow 0} \left(\frac{d\alpha}{dt}\right)_T = k_1 \quad (20)$$

Therefore, all of the k_1 values at different cure temperatures were obtained from Figure 3 by extrapolation to zero conversion. The results are listed in Table II. As can be seen, the higher the cure temperature, the larger the k_1 value.

Determination of reaction order, m , n , and rate constant k_2

After knowing the k_1 value, two linear equations were obtained by the rearrangement of eq. (14) into two different forms and followed by taking the logarithm

TABLE II
Kinetic Parameters of the Autocatalytic Model, $(d\alpha/dt) = (k_1 + k_2\alpha^m)(1 - \alpha)^n$, for Samples Cured at Different Temperatures

	Temperature (K)				
	513	523	533	543	553
$k_1 \times 10^3 \text{ (s}^{-1}\text{)}$	0.92	1.27	1.78	2.47	4.12
$k_2 \times 10^2 \text{ (s}^{-1}\text{)}$	0.82	1.27	1.76	2.28	3.53
m	1.07	0.98	0.94	1.01	0.97
n	0.89	0.97	1.03	1.08	1.05
$m + n$	1.96	1.95	1.97	2.09	2.02

$$\ln \left[\frac{\left(\frac{d\alpha}{dt}\right)_T}{(1-\alpha)^n} - k_1 \right] = \ln(k_2) + m \ln(\alpha) \quad (21)$$

$$\ln \left[\frac{\left(\frac{d\alpha}{dt}\right)_T}{k_1 + k_2\alpha^m} \right] = n \ln(1 - \alpha) \quad (22)$$

Because there were three unknown variables, m , n , and k_2 , they could not be solved directly by these two equations. An iteration method was therefore adopted, where an initial guess value of reaction order n was inserted into the left term of eq. (21). A linear plot was hopefully obtained from $\ln[(d\alpha/dt)_T/(1 - \alpha)^n] - k_1$ versus $\ln(\alpha)$ at each temperature, where the slope would be the reaction order m and the y -intercept would lead to the rate constant k_2 . The ob-

tained values of m and k_2 were then substituted into eq. (22) and another linear plot of $\ln[(d\alpha/dt)_T/(k_1 + k_2\alpha^m)]$ versus $\ln(1 - \alpha)$ was drawn. The slope was the new value of the reaction order n . This new n was again substituted into eq. (21) to obtain a new linear plot with a new set of m and k_2 values. The final values of m , n , and k_2 were obtained by repeating the above procedure, until these constants converged. For example, for the sample cured at 513 K, the initial guess value of n was 1.5 and the final converged values of m , n , and k_2 were 1.07, 0.89, and 0.82×10^{-2} (1/s), respectively. Figures 4 and 5 show the final converged linear plots of eqs. (21) and (22), for samples cured at different temperatures. The obtained reaction parameters, k_1 , k_2 , m , and n , are listed in Table II. The average values of m and n were 1.00 and 0.99, respectively, and the total reaction order was 1.99.

The activation energies E_1 and E_2 can be obtained from the slopes of two linear plots, namely, $\ln(k_1)$ versus $1/T$ and $\ln(k_2)$ versus $1/T$, respectively, from the Arrhenius equation, $k = A \exp(-E/RT)$. Figure 6 shows that a very good linear correlation was obtained for both plots. The calculated activation energies E_1 and E_2 were 80.90 and 82.31 kJ/mol, respectively. The total activation energy was about 163 kJ/mol. By substitution of the obtained values of k_1 , k_2 , m , and n into eq. (14), the theoretical curves of $d\alpha/dt$ versus α can be plotted. The theoretical curves fitted the experimental data very well, as shown in Figure 7.

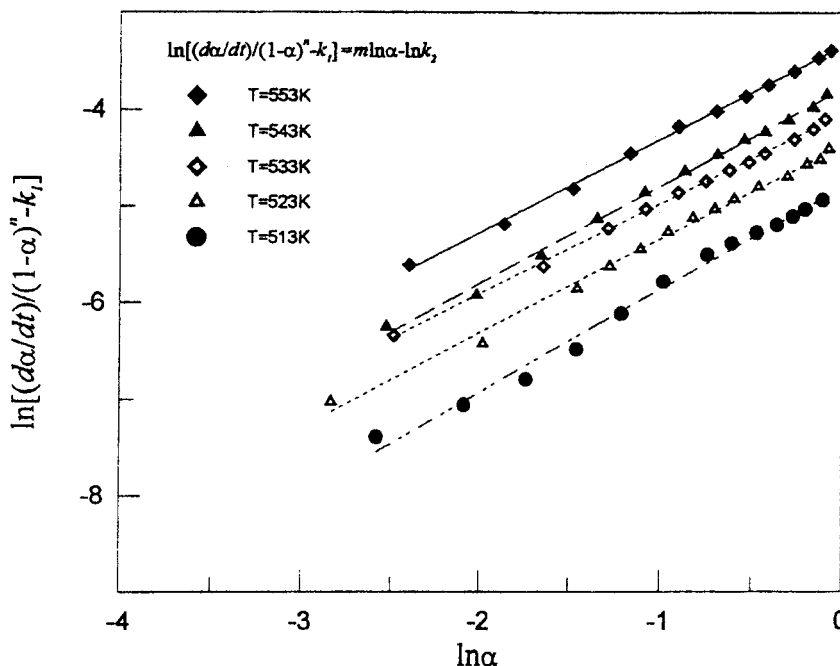


Figure 4 Final linear plots of $\ln[(d\alpha/dt)_T/(1 - \alpha)^n] - k_1$ versus $\ln(\alpha)$ by using Kenny's graphic-analytical technique to obtain kinetic parameters, m and k_2 , in the rate equation $d\alpha/dt = (k_1 + k_2\alpha^m)(1 - \alpha)^n$.

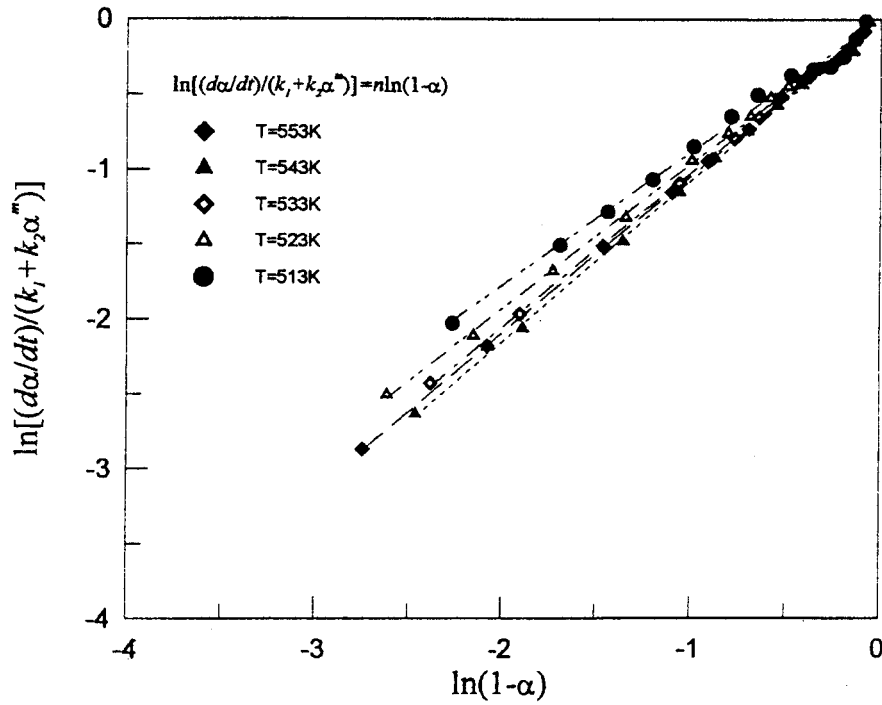


Figure 5 Final linear plots of $\ln[(d\alpha/dt)_T/(k_1 + k_2\alpha^n)]$ versus $\ln(1 - \alpha)$ by using Kenny's graphic-analytical technique to obtain kinetic parameter, n , in the rate equation $d\alpha/dt = (k_1 + k_2\alpha^n)(1 - \alpha)^n$.

Kenny's graphical analysis with a modified rate equation

Figure 7 shows that the kinetic model predicted the reaction rate became 0 at the complete conversion for

all samples, regardless of cure temperature. In the literature,^{16,27,28} when Kenny's graphic-analytical method was used to solve the kinetic parameters of eq. (14), the resin was generally assumed to be completely

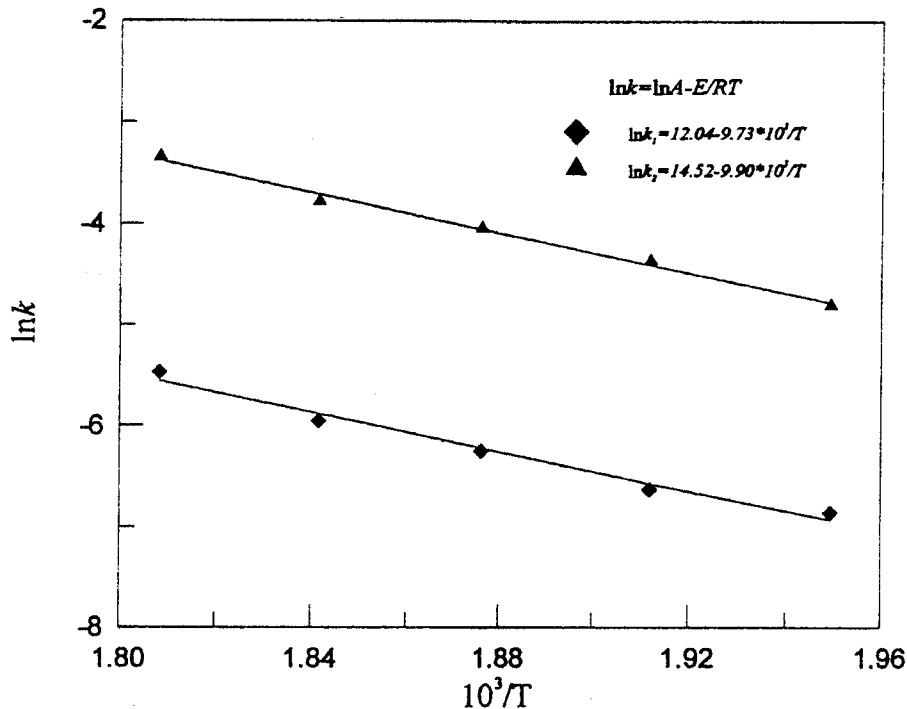


Figure 6 Temperature dependence of rate constants k_1 and k_2 from an autocatalytic model: $d\alpha/dt = (k_1 + k_2\alpha^n)(1 - \alpha)^n$. The two slopes were used to determine the activation energies E_1 and E_2 , respectively.

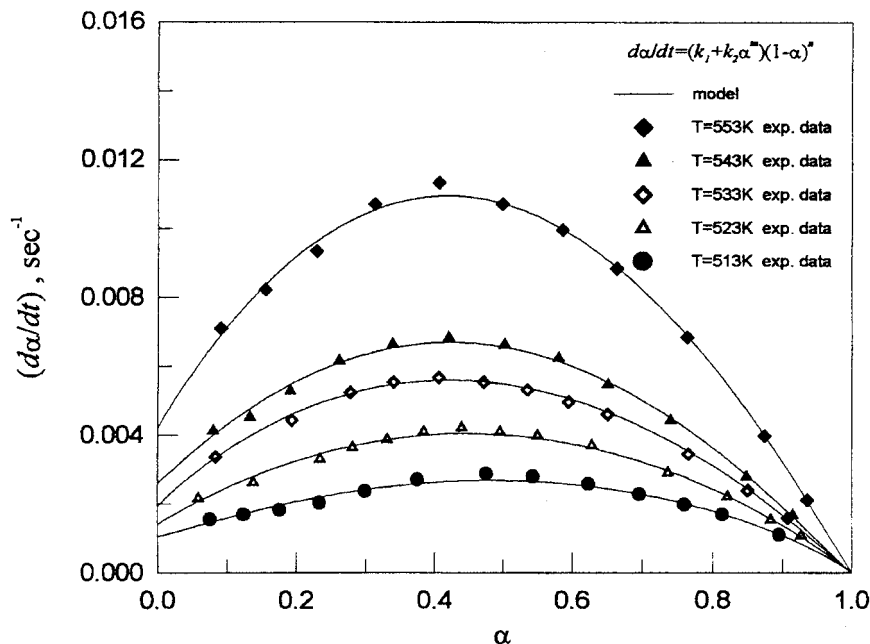


Figure 7 Comparison between model predictions and experimental data obtained from isothermal DSC tests at different temperatures. The model $d\alpha/dt = (k_1 + k_2\alpha^m)(1 - \alpha)^n$ assumes a complete conversion can be reached.

cured and the conversion could reach 1. The problem of limited mass transfer after gel formation was not considered. Actually, as the resin began to vitrify, no further reaction could occur. The maximum conversion was therefore less than 1. The conversion could only approach 1 at high cure temperatures. At low

cure temperatures, the cure behavior would deviate from eq. (14) after gelation. Torre and Kenny³⁸ used the autocatalytic model given by eq. (9) to describe the cure kinetics of epoxy and noticed the observed discrepancy between the model and experimental data at high conversions. Therefore, eq. (9) was modified to

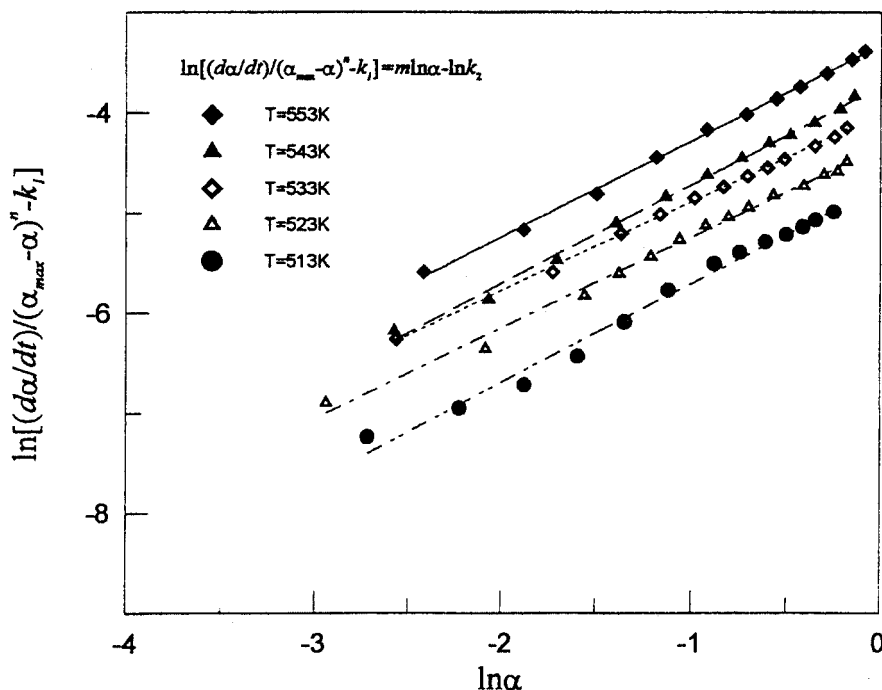


Figure 8 Final linear plots of $\ln[(d\alpha/dt)_T / (\alpha_{max} - \alpha)^n - k_1]$ versus $\ln(\alpha)$ by using Kenny's graphic-analytical technique to obtain kinetic parameters, m and k_2 , from a modified rate equation: $d\alpha/dt = (k_1 + k_2\alpha^m)(\alpha_{max} - \alpha)^n$.

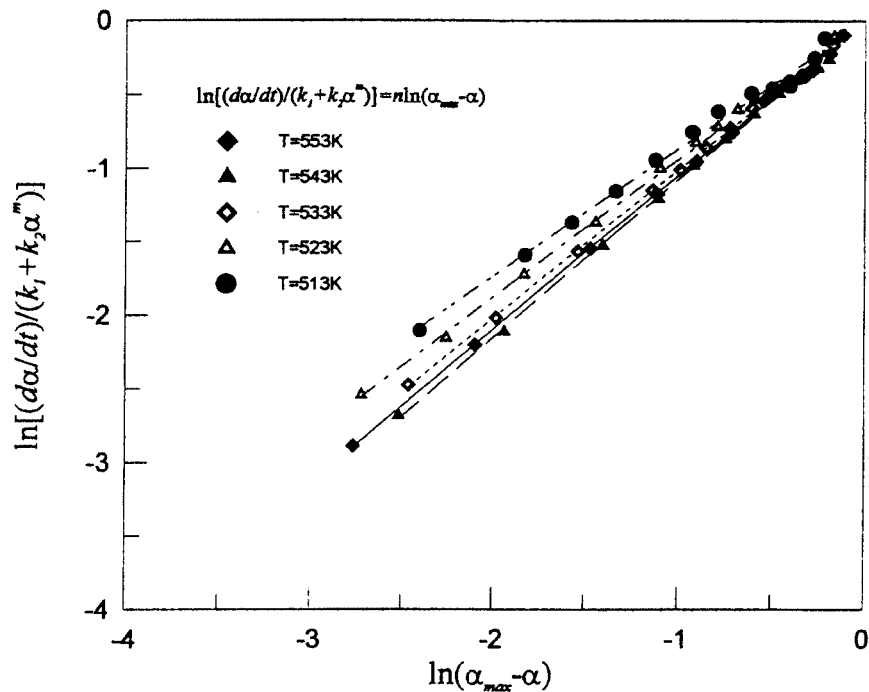


Figure 9 Final linear plots of $\ln[(d\alpha/dt)_T/(k_1 + k_2\alpha^m)]$ versus $\ln(\alpha_{\max} - \alpha)$ by using Kenny's graphic-analytical technique to obtain kinetic parameter, n , from a modified rate equation: $d\alpha/dt = (k_1 + k_2\alpha^m)(\alpha_{\max} - \alpha)^n$.

$$\frac{d\alpha}{dt} = k_2\alpha^m(\alpha_{\max} - \alpha)^n \quad (23)$$

where α_{\max} was defined as the largest attainable conversion. In this way, when $\alpha = \alpha_{\max}$, the reaction rate was equal to 0. Following Torre's concept, eq. (14) was now rewritten to yield

$$\frac{d\alpha}{dt} = (k_1 + k_2\alpha^m)(\alpha_{\max} - \alpha)^n \quad (24)$$

Similarly, eqs. (20), (21), and (22) were also changed to

$$\lim_{\alpha \rightarrow 0} \left(\frac{d\alpha}{dt} \right)_T = k_1\alpha_{\max}^n \quad (25)$$

$$\ln \left[\frac{\left(\frac{d\alpha}{dt} \right)_T}{(\alpha_{\max} - \alpha)^n} - k_1 \right] = \ln(k_2) + m \ln(\alpha) \quad (26)$$

$$\ln \left[\frac{\left(\frac{d\alpha}{dt} \right)_T}{k_1 + k_2\alpha^m} \right] = n \ln(\alpha_{\max} - \alpha) \quad (27)$$

With the above-modified equations, the same iteration method described previously was used to obtain the kinetic parameters, except that three equations were considered simultaneously instead of two. For exam-

ple, for the sample cured at 513 K with the same initial guess value of n , 1.5, the final converged values of k_1 , k_2 , m , and n were 1.06×10^{-3} (1/s), 0.89×10^{-2} (1/s), 0.96, and 1.05, respectively. Figures 8 and 9 show the final converged linear plots of eqs. (26) and (27), for samples cured at different temperatures. The obtained reaction parameters, k_1 , k_2 , m , and n , are listed in Table III. The average values of m and n were $0.95 (\pm 0.05)$ and $0.99 (\pm 0.09)$, respectively, where the number in parentheses was standard deviation. The total reaction order was 1.94. It was also observed that k_2 value was an order greater than the k_1 value. The ratio of k_2/k_1 was approximately 11 and this value almost did not change with cure temperatures from 513 to 553 K. This is not surprising, because neither metal ion nor any other external catalyst was added into the cyanate

TABLE III
Kinetic Parameters of the Autocatalytic Model, $(d\alpha/dt) = (k_1 + k_2\alpha^m)(\alpha_{\max} - \alpha)^n$, for Samples Cured at Different Temperatures

	Temperature (K)				
	513	523	533	543	553
$k_1 \times 10^3$ (s ⁻¹)	1.06	1.42	1.94	2.59	4.19
$k_2 \times 10^2$ (s ⁻¹)	0.89	1.31	1.83	2.40	3.61
k_2/k_1	11.9	10.8	10.6	10.8	11.6
m	0.96	0.99	0.89	0.91	0.99
n	1.05	1.08	1.01	0.94	0.87
$m + n$	2.01	2.07	1.90	1.85	1.86

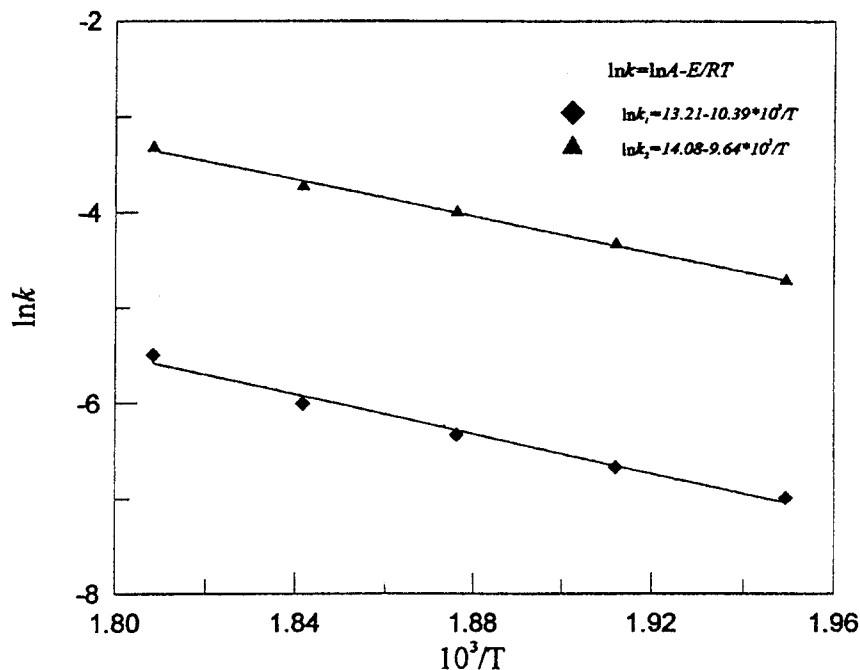


Figure 10 Temperature dependence of rate constants k_1 and k_2 from a modified kinetic model: $d\alpha/dt = (k_1 + k_2\alpha^m)(\alpha_{\max} - \alpha)^n$. The two slopes were used to determine the activation energies E_1 and E_2 , respectively.

ester resin in the current study. Therefore, the cure reaction was presumably dominated by the autocatalytic reaction.

In the literature,^{12,25,27} two sets of reaction orders for autocatalytic reactions of cyanate ester were most often cited. One of them, $n = 2$ and $m = 1$, was generally obtained by using spectroscopic methods such as Fourier transform infrared spectrophotometer.^{12,25} The other set, most often obtained from DSC, was $n = 1$ and $m = 1$, proposed by Kenny et al.,^{27,28} who developed the graphic-analytical method to calculate the reaction orders. However, complete cure was assumed in the model and therefore it was not applicable to samples cured at low temperatures. As a result, the reaction orders calculated from Kenny's study²⁸ were more scattering, although the average values were almost the same. The average values in Kenny's study were $m = 0.98 (\pm 0.12)$ and $n = 1.17 (\pm 0.18)$ for the samples isothermally cured at several temperatures ranging from 453 to 503 K.

The activation energies E_1 and E_2 for the new rate constants k_1 and k_2 were 86.38 and 80.15 kJ/mol, respectively, from the slopes of two linear plots shown in Figure 10. Again, a very good linear correlation was obtained for both plots. The total activation energy was about 166 kJ/mol, which was almost the same as the previous value from the model without modification. However, this value was a little higher than the values reported in the literature^{12,28,29} for various cyanate ester systems, 122–146 kJ/mol. This is probably because the cyanate ester monomer used in this study

was a novolac-type resin, which had a higher activation energy arising from the steric hindrance. By substitution of the obtained values of k_1 , k_2 , m , and n , into eq. (24), the theoretical curves of $d\alpha/dt$ versus α were plotted as shown in Figure 11. The theoretical curves fitted the experimental data very well even at high conversions. The reaction rate approached 0 at the maximum conversion where the resin was believed to begin vitrification. Equation (15), which described the cure time required to reach a certain conversion, was also changed to the following equation, accounting for the limited maximum conversion,

$$t = \int_0^{\alpha} \frac{d\alpha}{(k_1 + k_2\alpha^m)(\alpha_{\max} - \alpha)^n} \quad (28)$$

From the above equation with the known reaction parameters, the conversion (α) versus time (t) was plotted, as shown in Figure 12. A typical S-shaped curve was observed, consistent with characteristic of the autocatalytic reaction. The higher the cure temperature, the shorter the time to reach the maximum conversion, α_{\max} . In addition, the maximum conversion α_{\max} was dependent on the cure temperature in a manner that as the cure temperature was higher, α_{\max} was closer to unity.

CONCLUSION

In this study, DSC was used to investigate the cure kinetics of a novolac-type cyanate ester monomer,

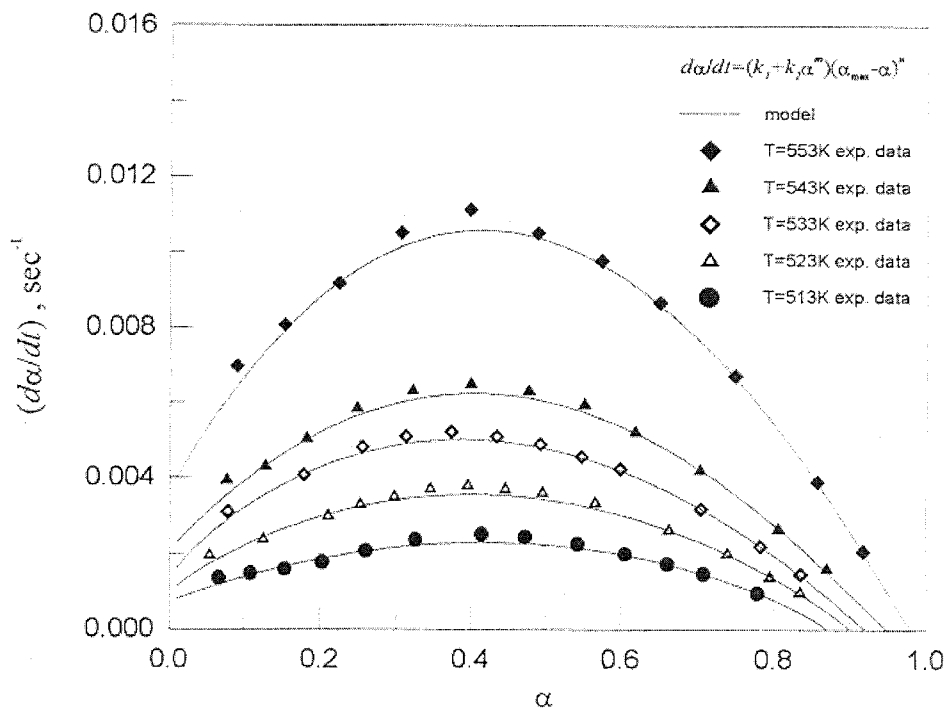


Figure 11 Comparison between model predictions and experimental data obtained from isothermal DSC tests at different temperatures. A modified kinetic model was used: $d\alpha/dt = (k_1 + k_2\alpha^m)(\alpha_{\max} - \alpha)^n$.

PT30. With the assumption that the heat of reaction was proportional to the conversion, the conversions and the reaction rates were calculated from the exo-

thermic curves at several isothermal temperatures (513–553 K). The plots of reaction rate versus conversion revealed an autocatalytic behavior. Considering

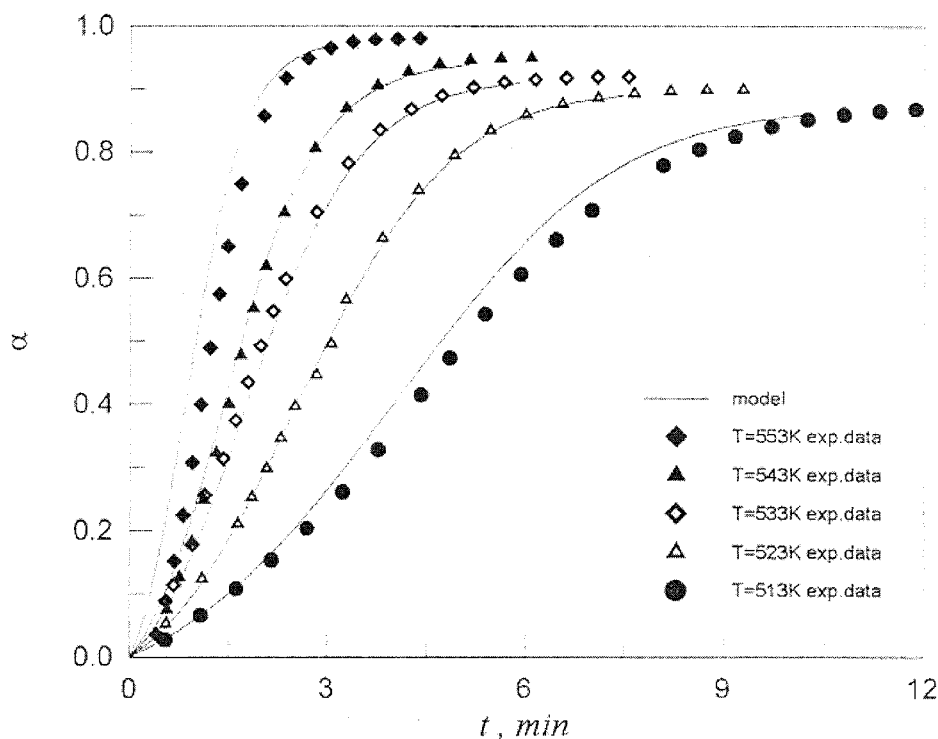


Figure 12 Comparison between model predictions and experimental data of conversion (α) with time, obtained from isothermal DSC tests at different temperatures. A modified kinetic model was used: $d\alpha/dt = (k_1 + k_2\alpha^m)(\alpha_{\max} - \alpha)^n$.

the problem of limited mass transfer after gel formation, a modified autocatalytic model was proposed, accounting for an incomplete conversion due to vitrification. By using Kenny's graphic-analytical technique, two reaction orders, m and n , and two rate constants, k_1 and k_2 , in the model for each cure temperature were obtained. By substituting these kinetic parameters into the model, the theoretical curves fitted the experimental data very well in the whole range of conversion. The overall reaction order was about 1.94 ($m = 0.95$, $n = 0.99$), and the activation energies for the rate constants, k_1 and k_2 , were found to be 86.4 and 80.2 kJ/mol. The total activation energy was about 166 kJ/mol, which was a little higher than the values reported in the literature. This is because the cyanate ester monomer used in this study was a novolac-type resin, which had a higher activation energy arising from the steric hindrance.

The authors express their appreciation for the financial support of the National Science Council, Taiwan, Republic of China (Project NSC 91-2622-E-032-001-CC3).

References

1. Hamerton, I. *Chemistry and Technology of Cyanate Ester Resins*, 1st ed.; Blackie Academic: New York, 1994; Chapter 1–2.
2. Kim, B. S. *J Appl Polym Sci* 1997, 65, 85.
3. Mathew, D. C.; Nair, P. R.; Ninan, K. N. *J Appl Polym Sci* 1999, 74, 1675.
4. Grenier-Loustalot, M.; Lartigau, C. *J Polym Sci, Part A: Polym Chem* 1997, 35, 3101.
5. Nair, C. P. R.; Francis, T.; Vijayan, T. M.; Krishnan, K. *J Appl Polym Sci* 1999, 74, 2737.
6. Nair, C. P. R.; Bindu, R. L.; Joseph, V. C. *J Polym Sci, Part A: Polym Chem* 1995, 33, 621.
7. Woo, E. M.; Su, C. C.; Kuo, J. F. *Macromolecules* 1994, 27, 5291.
8. Hedrick, J. L.; Russell, T. P.; Hedrick, J. C.; Hilborn, J. G. *J Polym Sci, Part A: Polym Chem* 1996, 34, 2879.
9. David, H.; Prevorsek, D. C. *Polym Eng Sci* 1985, 25, 804.
10. Bauer, M.; Bauer, J.; Kuhn, G. *Acta Polym* 1986, 37, 715.
11. Bauer, M.; Bauer, J. *Acta Polym* 1987, 38, 16.
12. Simon, S. L.; Gillham, J. K. *J Appl Polym Sci* 1993, 47, 461.
13. Keenan, M. R. *J Appl Polym Sci* 1987, 33, 1725.
14. Khanna, Y. P.; Kumar, R.; Das, S. *Polym Eng Sci* 1990, 30, 1171.
15. Khanna, U.; Chanda, M. *J Appl Polym Sci* 1993, 49, 319.
16. de la Caba, K.; Guerrero, P.; Mondragon, I.; Kenny, J. M. *Polym Int* 1998, 45, 333.
17. Salla, J. M.; Ramis, X. *Polymer* 1995, 36, 3511.
18. Shimp, D. A. (to Ciba-Geigy) U.S. Pat. 4,604,452, 1986.
19. Shimp, D. A. (to Ciba-Geigy) U.S. Pat. 4,608,434, 1986.
20. Shimp, D. A. (to Ciba-Geigy) U.S. Pat. 4,785,075, 1986.
21. Osei-owusu, A.; Martin, G. C. *Polym Eng Sci* 1991, 31, 1604.
22. Osei-owusu, A.; Martin, G. C. *Polym Eng Sci* 1992, 32, 535.
23. Osei-owusu, A.; Martin, G. C.; Gotro, J. T. *Polymer* 1996, 37, 4869.
24. Mathew, D.; Nair, C. P. R.; Ninan, K. N. *J Polym Sci, Part A: Polym Chem* 1999, 37, 1103.
25. Grenier-Loustalot, M.; Lartigau, C.; Metras, F.; Grenier, P. *J Polym Sci, Part A: Polym Chem* 1996, 34, 2955.
26. Kamal, M. R. *Polym Eng Sci* 1973, 13, 59; *Polym Eng Sci* 1974, 14, 231.
27. Zeng, S.; Ahn, K.; Seferis, J. C.; Kenny, J. M.; Nicolais, L. *Polym Comp* 1992, 13, 191.
28. Kenny, J. M. *J Appl Polym Sci* 1994, 51, 761.
29. Georjon, O.; Galy, J.; Pascault, J. *J Appl Polym Sci* 1993, 49, 1441.
30. Ryan, M. E.; Dutta, A. *Polymer* 1979, 20, 203.
31. Han, C. D.; Len, K. W. *J Appl Polym Sci* 1983, 28, 3155, 3185, 3207.
32. Riccardi, C. C.; Adabbo, H. E.; Williams, R. J. J. *J Appl Polym Sci* 1984, 29, 2481.
33. Cole, K. C.; Hechler, J. J.; Noel, D. *Macromolecules* 1991, 24, 3098.
34. Scott, E. P. *Polym Eng Sci* 1993, 33, 1157, 1165.
35. Chen, L. W.; Fu, S. C.; Cho, C. S. *Polym Int* 1998, 46, 325.
36. Simon, S. L.; Gillham, J. K. *Polym Prepr* 1991, 32, 182.
37. Kasehagen, L. J.; Macosko, C. W. *Polym Int* 1997, 44, 237.
38. Torre, L.; Kenny, J. M. *Proceeding of Twelfth Annual Meeting of Polymer Processing Society; Sorrento, Italy, 1996; p. 623.*